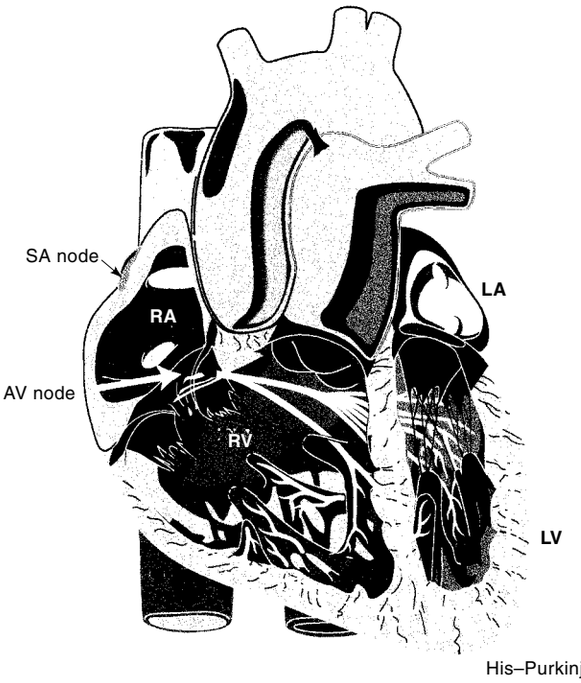

Figure 1. Diagram of the heart's electrical system. An electrical signal begins at the sino-atrial node (SA node) and travels to the left atrium (LA) and right atrium (RA). The signal also travels to the atrioventricular (AV) node. From the AV node, the electrical signal travels through the His–Purkinje system to the right ventricle (RV) and left ventricle (LV). The electrical signal causes the heart to contract in a coordinated fashion.

DEFIBRILLATORS

The function of the heart is to pump blood. The heart has two sides, each consisting of an atrium and a ventricle. Deoxygenated blood is collected in the right atrium, passed to the right ventricle, and pumped to the lungs where it is oxygenated. Blood is then collected in the left atrium, passed to the left ventricle, and pumped to the rest of the body. Controlling this pumping of blood is an electrical signal which passes through the heart and triggers a coordinated mechanical contraction of the heart. During a normal or sinus beat, this electrical activity starts in the sinus node, near the junction of the superior vena cava and right atrium, and passes through the right atrium to the atrioventricular node (Fig. 1). From there, the electrical signal spreads down the His bundle and throughout the left and right ventricles via a series of specialized conducting cells called Purkinje fibers. Mechanical action of the heart follows the same pattern with the atria contracting first and then the ventricles contracting second. The role of the Purkinje fibers is to rapidly spread the activation signal from the base to the apex of the heart so that contraction can proceed from apex to base, pushing blood out of the heart and into the aorta.

There are several disorders of this electrical system. Sometimes the heart beats too slowly, either because the sinus node does not fire rapidly enough, or the signal is not able to pass through the atrioventricular node to the ventricle. These problems are best treated with an implanted pacemaker. Sometimes, though, the heart beats too fast. A fast heart rhythm of any sort is called a tachyarrhythmia. If the heart is beating too fast but in an organized repeating fashion, the rhythm is called tachycardia. If the heart is beating too fast and in a disorganized fashion, the rhythm is called fibrillation. Either the atria or the ventricles can develop tachycardia or fibrillation. The danger of either tachycardia or fibrillation is that the heart is unable to pump enough blood to support the body. Tachycardias, both atrial and ventricular, as well as atrial fibrillation tend to be tolerated by patients while ventricular fibrillation is fatal in 5 min to 20 min unless corrected by defibrillation.

To date, the most effective treatment for atrial fibrillation and the only effective treatment for ventricular fibrillation is to apply a large electrical shock to the heart. Much research has been done to understand how this large electrical shock interacts with the heart to halt fibrillation. The first part of this article will discuss practical aspects of defibrillators and defibrillation: the most appropriate ways to measure defibrillation efficacy, the effect of electrode size and location, and the effect of waveform shape. The second part will discuss why an electrical shock is able to stop fibrillation and allow a regular rhythm to resume.

TYPES OF DEFIBRILLATORS

There are two main types of defibrillators used today, the automatic internal defibrillator and the external defibrillator.

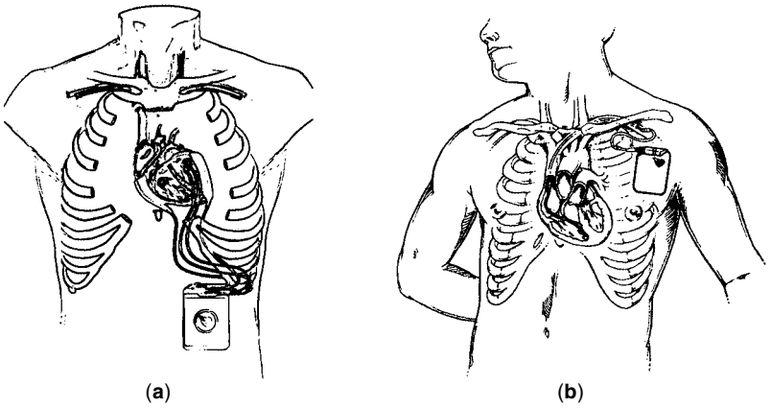

Figure 2. Diagram of an implantable cardiovertor defibrillator. The pulse generator is implanted in the pectoral region. A transvenous catheter electrode is threaded from the subclavian vein to the superior vena cava and into the right ventricle of the heart. This catheter also contains a pace/sense electrode on the tip. Implantation of this system only requires sedation of the patient and a local anesthetic.

The automatic internal cardiovertor-defibrillator (ICD) is a 40 mL to 100 mL box with electrodes attached to it that extend either onto the epicardial (outside) surface of the heart or into the chambers of the heart (Fig. 2). This device monitors the cardiac rhythm and if ventricular fibrillation is detected delivers a strong electrical shock, usually 10 J to 30 J. Currently, implantation of an ICD is the treatment of choice for patients who have survived an initial episode of sudden cardiac death and do not have a treatable cause for their arrhythmia. (1,2).

The external defibrillator is a device distributed throughout the prehospital and hospital setting (the paddles popularized in television hospital dramas). These devices deliver a large electric shock, usually 100 J to 360 J, to the chest wall of a patient via either hand-held paddle electrodes or self-adhesive patch electrodes (Fig. 3). The external defibrillator is used to stop both ventricular and atrial tachyarrhythmias. Traditionally, the external defibrillator operator has analyzed the patient's heart rhythm and decided whether or not to deliver the electrical shock. Newer devices, intended to be used by minimally trained lay persons, such as police, firefighters, flight attendants, or even passers-by, will analyze the patient's heart rhythm and determine whether or not a shock should be delivered without intervention from the operator. Perhaps someday defibrillators will be as common as fire extinguishers. Quick action is vital to the survival of ventricular fibrillation. The rate of survival following an episode of ventricular tachycardia/ventricular fibrillation is inversely related to the time that the patient's heart has been in that rhythm before a shock is delivered (Fig. 4). Therefore, it is hypothesized that more patients would be saved if defibrillation occurred as soon as possible by individuals likely to be near the person when his/her heart fibrillates (3).

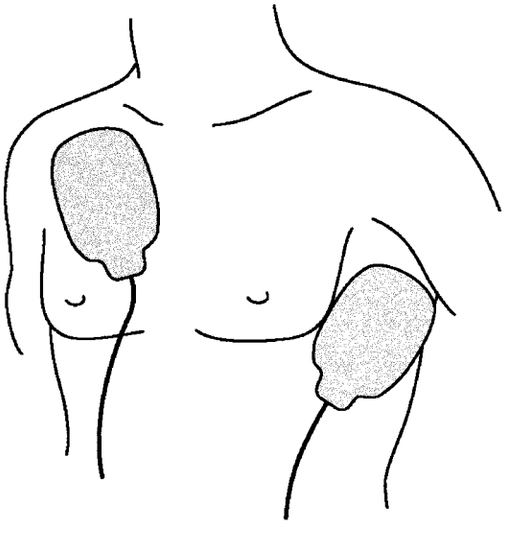

Figure 3. Diagram of electrode patch placement for external defibrillation. One electrode is placed over the right border of the sternum. The second electrode is placed on the left axillary line overlying the apex of the heart.

MEASURING DEFIBRILLATION EFFICACY

Whenever a defibrillation shock is delivered to a patient, the goal is to stop the tachyarrhythmia by stopping the heart completely, thereby allowing the patient's heart to resume beating with a slow regular rhythm. Therefore, to compare whether one defibrillator is better than another, it is necessary to be able to define the efficacy of a defibrillator. Although people describe defibrillation in terms of a threshold, it is more appropriately described as a probability function. Within a certain range, as the strength of the defibrillation

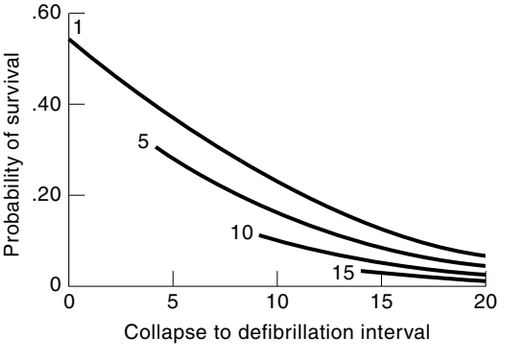

Figure 4. Probability of survival as a function of time in minutes from collapse to the beginning of cardiopulmonary resuscitation and time of defibrillation. Each contour represents a different time interval from collapse to the beginning of cardiopulmonary resuscitation. Note that the probability of survival from cardiac arrest drops as the time from arrest to the beginning of cardiopulmonary resuscitation increases and as the time to defibrillation increases. Reproduced with permission from the American Heart Association (98).

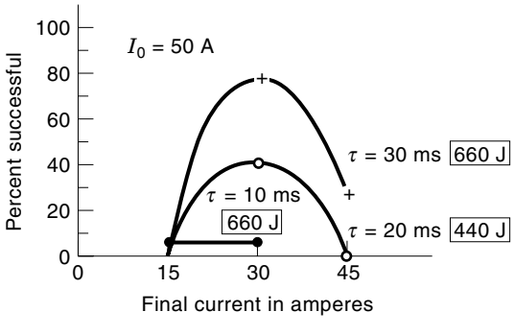

Figure 5. Relationship between percent success of ventricular defibrillation and final current for exponential waveforms having an initial current (I_0) of 50 A and time constants of decay (t) of 10, 20, and 30 ms. Energy is shown in joules for each time constant of decay (t). Reproduced with permission from The Institute of Electrical and Electronics Engineers (99).

shock increases, the probability increases that the shock will defibrillate the heart (Fig. 5) (4). This increase is plotted as a *probability of success curve.* Defining a probability of success curve requires a large number of shocks, 10 to 15, and so it is impractical to always determine the entire curve for each patient. Therefore, several methods to estimate the 50% point of the probability of success curve have been developed, including the step down (5), up/down (6), and the binary search (7). All of these methods are described as *measuring the defibrillation threshold* in the literature. With the step down technique, the first shock delivered is of a strength that almost always defibrillates. Then progressively smaller shocks are delivered until a shock fails to defibrillate the heart. The up–down technique starts at a particular shock level, one thought to be close to an estimated 50% success level, and shocks are delivered at progressively higher or lower shock levels depending on the result of the previous trial until a reversal from success to failure or failure to success occurs (8). The binary search algorithm chooses a range in which the defibrillation threshold is thought to be, generally 0 J to 20 J (7). The first shock is delivered in the center of the search space. If the shock succeeds, then the next shock strength is the middle of the lower half of the initial search space. If the shock fails, the next shock strength is the middle of the higher half of the initial search space. The search space is progressively bisected until the desired level of precision is reached.

These methods of estimating the 50% defibrillation success level are sensitive to decisions made by the operator and underlying biases introduced by the algorithm itself. The binary search algorithm requires that the operator estimate a range that the defibrillation threshold is within. If the defibrillation threshold is not within the range, then the algorithm will never converge on an answer. The step-down method tends to overestimate the 50% success point. A step size that is too small for a step-down or up–down method requires an excessive number of shocks to determine the 50% success point. If the step size is too large, the precision of the estimate becomes very low. Empirically, people have used energy step sizes of approximately 10% to 20%. McDaniel and Schuder suggest that a log(energy step) equal to 0.05 is the best choice (6). They base this on their laboratory data, which suggests

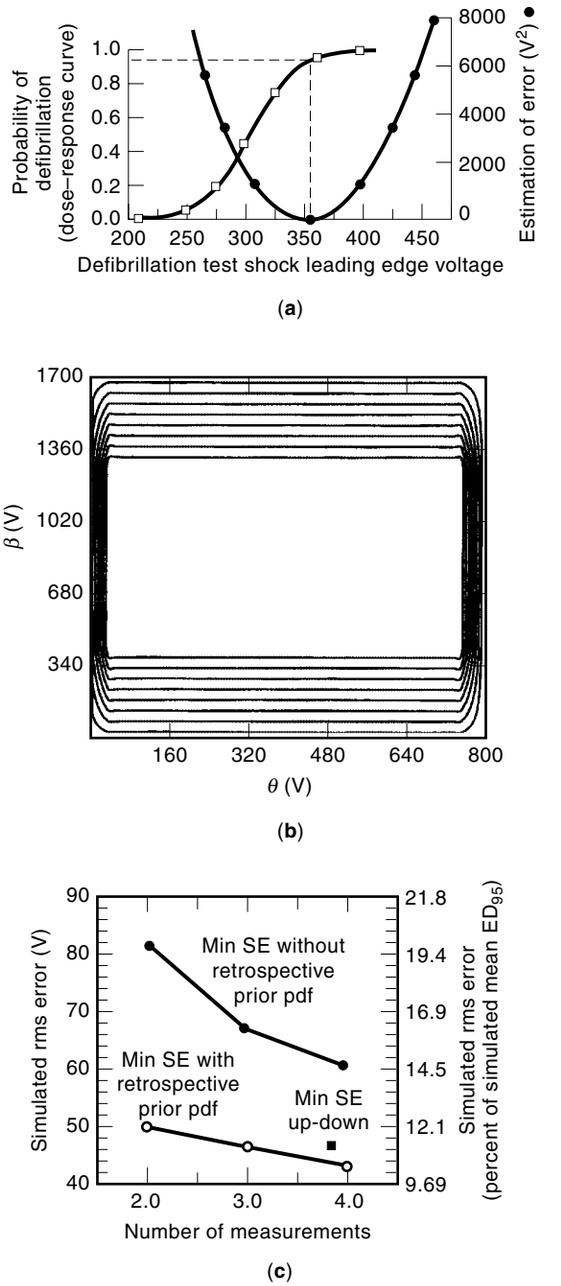

Figure 6. A Bayesian approach to estimating the 95% probability of successful defibrillation. (a) The method assumes a dose–response curve (open squares) which follows the logistic equation, although any functional form could be used. Also shown is the cost function (closed circles) that was chosen to give the lowest error. Cost functions that minimize the absolute error or the patient risk are also possible. (b) Contour plot of a prior probability density function (pdf) constructed from a set of assumptions applicable to most implantable defibrillator electrode configurations. θ and β are variables that describe the logistic equation at the 95% probability point. θ is the subject's 95% probability point. One over β is the slope of the logistic equation at the 95% probability point. For any animal, it is assumed that the 95% probability point will be between 0 V and 800 V (θ) and that one over the slope of the logistic equation (β) is between 0 V and 1700 V. (c) The simulated performance of the minimum squared error (MinSE) developed from (a) and (b).

that one standard deviation of the threshold is approximately log(0.05) energy units.

A less widely used but promising method of estimation has been developed by Malkin et al. (9). Bayesian estimation techniques are used to estimate both 50 and 95 points of the probability of success curve in a given patient (Fig. 6) (9,10). By making several conservative assumptions about the probability search space and using a variable step sizes, Malkin et al. showed that the 95% success level can be estimated with a root mean square error of 15% (10). Although estimating the 50% success level is valuable in the research laboratory, estimating the 95% success level in patients would allow the physician implanting an ICD to set appropriate shock treatment strengths with a great deal of confidence and so this methodology holds great promise.

EFFECT OF ELECTRODE SIZE AND LOCATION ON DEFIBRILLATION EFFICACY

So far, we have discussed how to measure the efficacy of a defibrillator by estimating some point on the probability of success curve. In the next two sections we discuss some of the factors that affect efficacy.

The electrodes that deliver the shock have a large effect on defibrillation efficacy. The different forms of defibrillators deliver electric shocks from different size electrodes that are positioned on different parts of the body. ICDs initially delivered shocks to the ventricles of the heart from either two patches on the epicardial surface of the heart [Fig. 1(a)] or a patch on the left ventricular epicardium to a coil electrode in the superior vena cava-right atrium. These electrode configurations had 10 J to 34 J defibrillation thresholds using monophasic waveforms. With the development of biphasic waveforms, it became possible to shock from a coil electrode in the right ventricle to a coil in the superior vena cava-right atrium with or without a patch on the left chest wall. This change allowed patients to undergo implantation of an ICD without the risk associated with a thoracotomy. Even more recently, with the advent of smaller devices and the ability to implant them in the pectoral region, the metallic shell of the device has been used as the return electrode for a coil electrode in the right ventricle [Fig. 1(b)]. With all of these electrode configurations, almost 100% of patients will have a defibrillation threshold or estimated ED_{50} of less than 24 J if a biphasic waveform is used (11).

Automatic internal atrial defibrillation is now being performed as an investigational technique. Currently, the best electrode configuration for atrial defibrillation is a coil electrode in the right atrium and a second coil electrode in the coronary sinus underlying the left atrial appendage (12). With a biphasic waveform, atrial defibrillation thresholds vary from 1.5 J to 10 J (13–15). Unfortunately, the pain threshold for patients with implanted atrial defibrillators is thought to be less than 1 J (16), although the pain threshold has been shown to be highly variable within a given patient and from patient to patient. Newer techniques that use multiple electrodes and sequential shock delivery have lowered the atrial defibrillation threshold significantly (17).

Shocks delivered from the body surface typically require 200 J to 360 J for a damped sinusoidal waveform (18), although recent evidence suggests that biphasic waveforms may require less energy (19,20). Because only approximately 4% to 20% of the current delivered by transthoracic defibrillation electrodes ever reaches the heart, energy requirements for external defibrillation greatly exceed the energy required for internal defibrillation (21–23).

THE EFFECT OF WAVEFORM SHAPE ON DEFIBRILLATION EFFICACY

An understanding of how the magnitude and shape of the waveform effects efficacy is vital to understanding defibrillators and defibrillation. Traditionally, the efficacy of defibrillation waveforms has been measured in terms of energy. Using energy as a measure of the efficacy of the defibrillation is very useful when determining the engineering requirements of a defibrillator, such as how big the components need to be or the relative efficacy of different defibrillator waveform-electrode configurations. Several studies, however, have shown that current may be a better measure of a defibrillation waveform's efficacy (24,25). These studies have shown that, although the amount of energy necessary to defibrillate a patient varies from individual to individual, the current necessary to defibrillate remains relatively constant.

Variations in waveform shape have a large effect on a defibrillator's ability to halt fibrillation. Currently, two different waveform types are used clinically: monophasic and biphasic (Fig. 7). In a monophasic waveform, the voltage on each electrode remains either positive or negative for the duration of the entire waveform. In a biphasic waveform, the voltage on the electrodes reverses part way through the duration of the waveform. Within each type, waveforms can be described as truncated exponential or damped sinusoidal. Most ICDs use biphasic truncated exponential waveforms. In contrast, most external defibrillators to date have employed damped sinusoidal monophasic waveforms. Because of the inductor necessary to shape the damped sinusoidal waveform, these defibrillators tend to be large and heavy. More recently, smaller, lighter

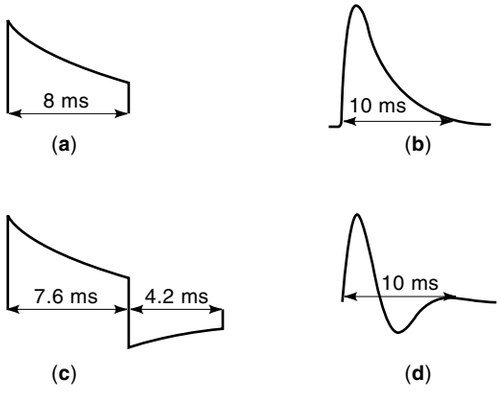

Figure 7. Some of the different waveform shapes used in clinically available defibrillators. (a) Truncated exponential monophasic waveform. This waveform is used in older ICDs. (b) Damped sinusoidal monophasic waveform. This waveform is used in a majority of external defibrillators in use today. (c) Truncated exponential biphasic waveform. This waveform is used in ICDs currently being implanted and in newly available external defibrillators. (d) Damped sinusoidal biphasic waveform. This waveform is used in external defibrillators used in Russia (100).

external defibrillators have been developed that employ truncated exponential biphasic waveforms, similar to those used in ICDs (19,26)

Many studies have shown that certain biphasic waveforms defibrillate with a lower current and energy than a monophasic waveform. It is important to choose the relative phase durations of the two phases of the biphasic waveform carefully in order to realize an improvement in efficacy over the monophasic waveform. For waveforms with long time constants, the first phase should be longer than or equal to the second phase (27,28). For waveforms with a short time constant, the second phase can be slightly longer than the first phase (29–31).

Several groups have shown that for square waveforms, defibrillation efficacy follows a strength–duration relationship similar to cardiac stimulation (32,33); as the waveform gets longer, the average current at the 50% success point becomes progressively less, approaching an asymptote called the rheobase (34). Based on this observation, several groups have suggested that cardiac defibrillation can be mathematically modeled using a parallel resistor–capacitor (*RC*) network to represent the heart (Fig. 8) (29,35–37). Empirically, it has been determined that the time constant for the parallel *RC* network is in the range of 2.5 ms to 5 ms (29,31,36). In one version of the model (29), a current waveform is applied to the *RC* network. The voltage across the network is then calculated for each time point during the defibrillation pulse. The relative efficacy of different waveform shapes and durations can be compared by determining the current that is necessary to make the voltage across the *RC* network reach a particular value, called the defibrillation threshold.

Several observations can be made from this model. First, for square waves, as the waveform duration gets longer, the voltage across the network gets progressively higher and approaches an asymptote or rheobase. For truncated exponential waveforms, however, the model voltage rises, reaches a peak, and then, if the waveform is long enough, begins to decrease (Fig. 8). Therefore, the model would predict that monophasic exponential waveforms should be truncated at a time when the peak voltage across the *RC* network is reached. Current or energy delivered after that time is wasted and may even be detrimental if the waveform gets too long (38). In supporting this prediction, strength–duration relationships measured in both animals (29) and humans (39) do not approach an asymptote but reach a minimum and remain there as the waveform gets longer.

Secondly, the model predicts that the heart acts as a low-pass filter (37). Therefore waveforms that rise gradually should have an improved efficacy over waveforms that turn on immediately. This prediction has been shown to hold true for external defibrillation (40), internal atrial defibrillation (41), and internal ventricular defibrillation (42). Ascending ramps defibrillate with a greater efficacy than do descending ramps (42,43). Sweeney et al. showed that a square wave duty cycle waveform (a waveform in which the current is rapidly turned on and off) defibrillates with the same efficacy as a square waveform delivering the same total charge as the duty cycle waveform (37). This idea has implications for new defibrillators that would use a duty cycle concept to shape a waveform.

Several groups have suggested that the optimal first phase of a biphasic waveform is the optimal monophasic waveform

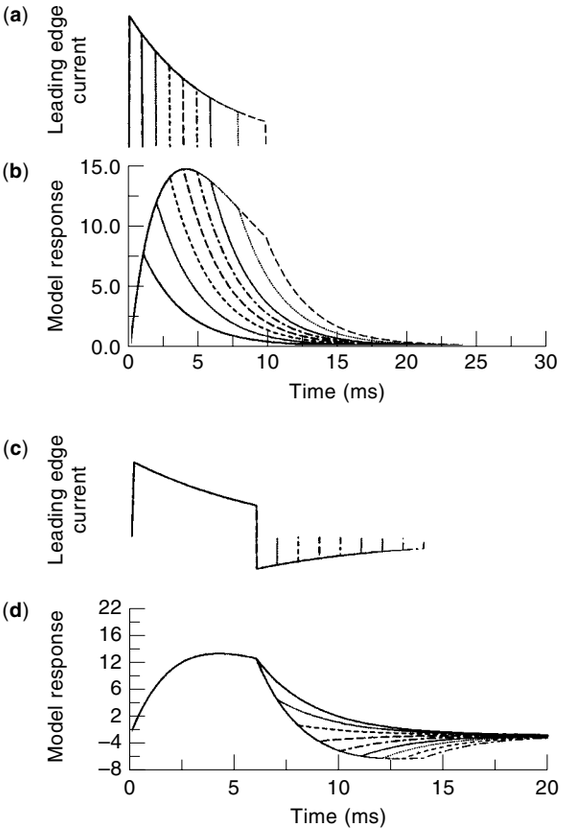

Figure 8. The response of a parallel resistor–capacitor network representation of the heart to a monophasic and biphasic truncated exponential waveform with a time constant of 7 ms. The parallel resistor–capacitor network has a time constant of 2.8 ms. (a) Input monophasic waveforms. Leading edge current of the input waveform was 10 A. The waveforms were truncated at 1, 2, 3, 4, 5, 6, 8, and 10 ms. (b) Model response, $V(t)$. Initially, as the waveform gets longer, $V(t)$ increases until it reaches a maximum at approximately 4 ms, after which $V(t)$ begins to decrease. (c) Input biphasic waveforms. Leading edge current was 10 A. Phase 1 was truncated at 6 ms. Phase 2 was truncated after 1, 2, 3, 4, 5, 6, 7, and 8 ms. (d) The model response does not change polarity until phase 2 duration is longer than 2 ms.

(30,44). If this is true, then what does the model predict to be the best second phase of a biphasic waveform? Empirically, it seems that the role of the second phase is to return the model voltage response as closely to zero as quickly as possible in order to maximize the increased efficacy of the biphasic waveform over that of the monophasic waveform with the same duration as phase one of the biphasic waveform. If the network voltage does not reach zero, or it overshoots zero, then efficacy is lost (29,30). Swerdlow et al. have shown in humans that the best second phase of a biphasic waveform is one that returns the model response close to zero (31).

Together, these ideas allow one to optimize capacitor sizes and phase durations for truncated exponential biphasic waveforms, the most commonly used waveforms in ICDs. The capacitor has to be large enough to be able to raise the network voltage to its threshold value and still be able to hold enough charge to drive the network voltage back to zero. For a 40 Ω interelectrode impedance and a network time constant of 2.8

ms, the minimum capacitor size that can accomplish this is 75 μF.

Only a few studies have examined the effects of the duration of fibrillation on the defibrillation threshold. Most of these studies deal with internal defibrillation and with fibrillation durations of less than one minute (45–47). In a dog model of defibrillation, using internal electrodes and bidirectional monophasic defibrillation pulses delivered along two pathways, Echt et al. showed that the energy necessary to defibrillate rose from 27 ± 13 J at 5 s of fibrillation to 41 ± 14 J at 30 s of fibrillation (45). Jones et al. showed that in a working rabbit heart model of defibrillation both monophasic and biphasic waveform defibrillation thresholds increased with duration from 5 to 15 to 30 s (47). At all durations, the biphasic threshold was lower than the monophasic threshold. This difference increased with fibrillation duration. In a study using sequential trapezoidal defibrillation pulses in a pig model of defibrillation, Fujimura et al. concluded that a delay in defibrillation therapy of up to 90 s has no significant effect on the ability to defibrillate the heart (48). Bardy et al. found no difference between the mean defibrillation thresholds in humans when fibrillation was allowed to continue for 10 versus 20 s (11.5 ± 5.9 J versus 12.0 ± 6.9, p = NS) (46). Winkle et al. showed that in humans the probability of successful defibrillation with low energy shocks (5.9 J) was higher for ventricular fibrillation lasting 5 s than for ventricular fibrillation lasting 15 s, yet there was no significant difference between the success rates of high energy shocks (24.2 J) delivered at the same two durations (49). Together, these results suggest that for ventricular fibrillation durations up to 90 s, the defibrillation threshold for monophasic waveforms increases with duration while the results are inconclusive for biphasic waveforms.

MECHANISMS OF DEFIBRILLATION

In the following sections, the interaction between the defibrillation shock and the fibrillating myocardium will be discussed. We start with how the distribution of the current from the shock affects defibrillation. Then we discuss how the shock interacts with the fibrillating myocardium. Finally, we discuss how the shock changes the action potential, the transmembrane potential, and the ion channels in the membrane. By looking at all of these different shock–fibrillating heart interactions, we will attempt to summarize what is known about how an electrical shock causes the fibrillating heart to return to sinus rhythm.

Potential Gradient

During a shock, different amounts of current flow through different parts of the heart. According to Ohm's law, the current density through each region of the heart is equal to the potential gradient in that region divided by the resistivity of that region. Although current density is difficult to measure directly, techniques to measure the potential gradient are well established. If we make the assumption that tissue resistivity is constant in the heart, then the potential gradient is directly related to current density. For shocks delivered from intracardiac electrodes, the distribution of potential gradients is highly uneven. High potential gradients occur near the defibrillation electrodes. Low potential gradients occur distant from the defibrillation electrodes (Fig. 9). Just as there is a minimum shock strength needed to defibrillate consistently, it has been found that there is a minimum potential gradient that must be created throughout the ventricles by the shock to defibrillate consistently (50). The shock strength needed to defibrillate can vary widely for different defibrillation electrode configurations; however, the minimum potential gradient that must be created throughout the heart for a particular shock waveform is approximately the same even when the defibrillation electrode configuration is altered (50,51). This finding suggests that the minimum potential gradient generated throughout the heart by the shock is a more fundamental unit involved in the mechanism of defibrillation than is the shock strength delivered to the electrodes. Yet the minimum potential gradient necessary for defibrillation is different for different waveforms. For example, it is approximately 6 V/cm for a typical monophasic waveform, but is approximately 4 V/cm for a typical biphasic waveform (51). There-

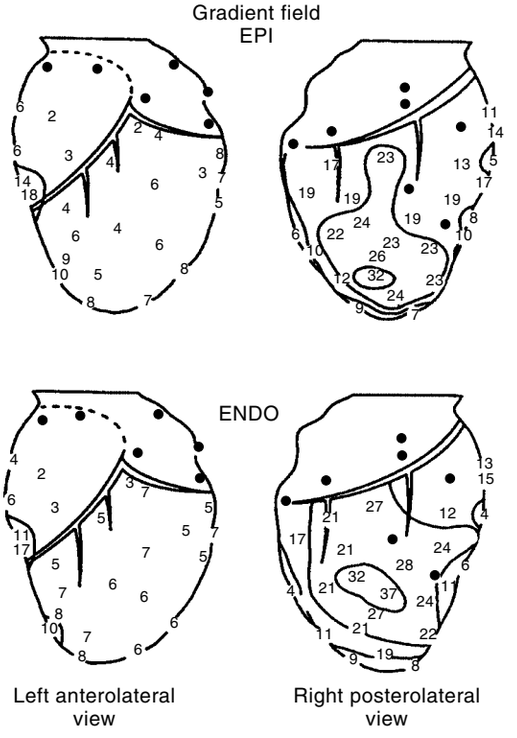

Figure 9. The potential gradient field from a 500 V, 6 ms unsuccessful defibrillation shock delivered from a catheter electrode in the right ventricular apex as cathode and a cutaneous patch on the lower left thorax as anode. Left-hand panels demonstrate the heart from the left anterolateral view; the two right-hand panels represent the right posterolateral angle. Numbers represent the potential gradient in volts per centimeter. Isogradient lines are separated by 10 V/cm. (Dashed line) The upper border of the right ventricular outflow tract. (Asterisks) The top row of electrodes in the atrium and right ventricular outflow tract where potential gradients could not be calculated because no recording sites were above them. Neighboring electrodes are required to calculate the potential gradient, defined as the change in potential with distance. (Solid circles) Electrodes from which good recordings were not obtained. (EPI) epicardial, (ENDO) endocardial. Reproduced with permission from The Institute of Electrical and Electronics Engineers (101).

fore, at this level of consideration of the mechanism of defibrillation, one of the reasons that some biphasic waveforms require a smaller shock than some monophasic waveforms for defibrillation is that they must create a lower minimum potential gradient throughout the heart.

Activation Sequence

There are two things that a shock must do in order to defibrillate the heart. First, it must stop all the fibrillation wavefronts on the heart. Second it must not restart fibrillation. When shocks are given that are much lower than the strength needed to defibrillate, activation after the shock appears at numerous sights throughout the ventricles (52). As the shock strength is increased, the potential gradients are increased throughout the myocardium, and activation originates just in those regions in which the potential gradients are lowest. For shocks just slightly lower than the strength needed to defibrillate, postshock activation arises only in the small myocardial regions in which the potential gradients remain below the minimum needed for defibrillation (Fig. 10). Activation fronts arising from these low potential gradient regions propagate to activate the remainder of the myocardium for a few cycles following the shock. Then reentry occurs, activation becomes disorganized, and the heart begins to fibrillate again. Following shocks slightly stronger than that needed to defibrillate, postshock sites of early activation still arise in the regions of lowest potential gradient; however, successive cycles of activation originate from these regions more slowly than following unsuccessful, slightly lower strength shocks. After a few cycles, these activations terminate without reinducing fibrillation (52,53). These results suggest that the reason a minimum potential gradient is required for defibrillation is that, above this minimum, activation fronts are not generated by the shock that can interact and reinduce fibrillation (53). For shocks delivered through transvenous electrodes at strengths a few hundred volts higher than needed to defibrillate, ectopic activation fronts first appear following the shock in regions exposed to the highest potential gradients generated by the shocks, adjacent to the defibrillation electrodes (54,55). In a similar fashion to activation fronts arising following shocks just above the defibrillation threshold, these activation fronts also terminate without reinitiating fibrillation. However, when the shock strength is increased still further, e.g. to above 1000 V with transvenous electrodes, the activation fronts arising from the high potential gradient regions can reinduce ventricular fibrillation, so that the shock fails even though a lower strength shock succeeds.

Cellular Action Potential

One effect of the shock field is to initiate a new action potential [Fig. 11(a)]. If the shock strength is large enough, new action potentials can be generated both in tissue adjacent to the defibrillation electrodes, and in regions throughout the myocardium distant from the defibrillation electrodes (56,57). Under certain conditions, the shock can have a second effect on the action potential. It can cause prolongation of the action potential and, as a result, a prolongation of the refractory period, without giving rise to a new action potential [Fig. 11(b)]. This action potential prolongation, called a graded response by some (58), occurs if a shock of sufficient strength is given when the cells are in their refractory period. Action potential prolongation occurs when the shock potential gradient delivered to the tissue is above the minimum level needed to defibrillate. At shock strengths less than the minimum needed to defibrillate, only an all-or-none response is observed [Fig. 4(a)] (59,60). Although these effects are important for electrical induction of reentry, the fact that action potential prolongation occurs in response to shock field strengths that occur during defibrillation suggests that action potential prolongation may also be important for defibrillation (59,61–65). Action potential prolongation and, hence, refractory period extension are hypothesized to play two different roles in the mechanism of defibrillation. One, they are thought to prevent the appearance of propagating activation fronts following the shock (52,66). Two, by causing a more uniform dispersion of refractoriness following the shock, they are thought to prevent the block and reentry that cause the activation fronts that do appear following the shock from degenerating into fibrillation (61–65).

In regions in which the shock potential gradient is high, over 50 V/cm to 70 V/cm, the shock can have detrimental effects, probably by causing electroporation of the cardiac cell membranes (67,68). This can cause the transmembrane potential to temporarily hang up near the value of the plateau of the action potential (69). The cell is electrically paralyzed and cannot conduct an action potential during this time. At yet higher potential gradients, probably over 150 V/cm, the exposed myocardium gives rise to arrhythmic beats (50). This may be the mechanism that causes the probability of the defibrillation success curve to decrease for very large shocks (Fig. 5).

Waveform shape alters the shock strength at which these detrimental effects on the myocardium occur. Yabe et al. showed that for a 10 ms truncated exponential monophasic waveform, conduction block occurred in dogs in regions where the potential gradient was greater than $64 \pm 4\ \mathrm{V \cdot cm^{-1}}$ (70). Conduction block would last longer for shocks that created even higher potential gradients in the myocardium. In contrast to monophasic shocks, conduction block occurred when the potential gradient in the myocardium reached 71 ± 6 V/cm for a 5 ms/5 ms truncated exponential biphasic shock. Jones et al. showed that adding a second phase to a monophasic waveform (i.e., making it a biphasic waveform) decreased the damage done to cultured chick myocytes by the monophasic waveform alone (71). Both results show that biphasic waveforms are less apt to cause damage or dysfunction in high-gradient regions. The therapeutic index has been defined as the range of energies over which a defibrillation waveform is both safe and effective. Since biphasic waveforms defibrillate at lower energies and cause more myocardial damage than monophasic waveforms, they have been described as having a higher therapeutic index than monophasic waveforms.

Transmembrane Potential

For the shock to cause either a new action potential to be triggered or to prolong an action potential, it must alter the transmembrane potential. It has been estimated that only about one quarter of the total current traversing the heart crosses the membrane to enter the cells (72). Since the defibrillation electrodes are located extracellularly, current from the shock that enters myocardial cells in some regions must exit the cells in other regions. These currents, which flow through the cell membrane, will introduce changes in the

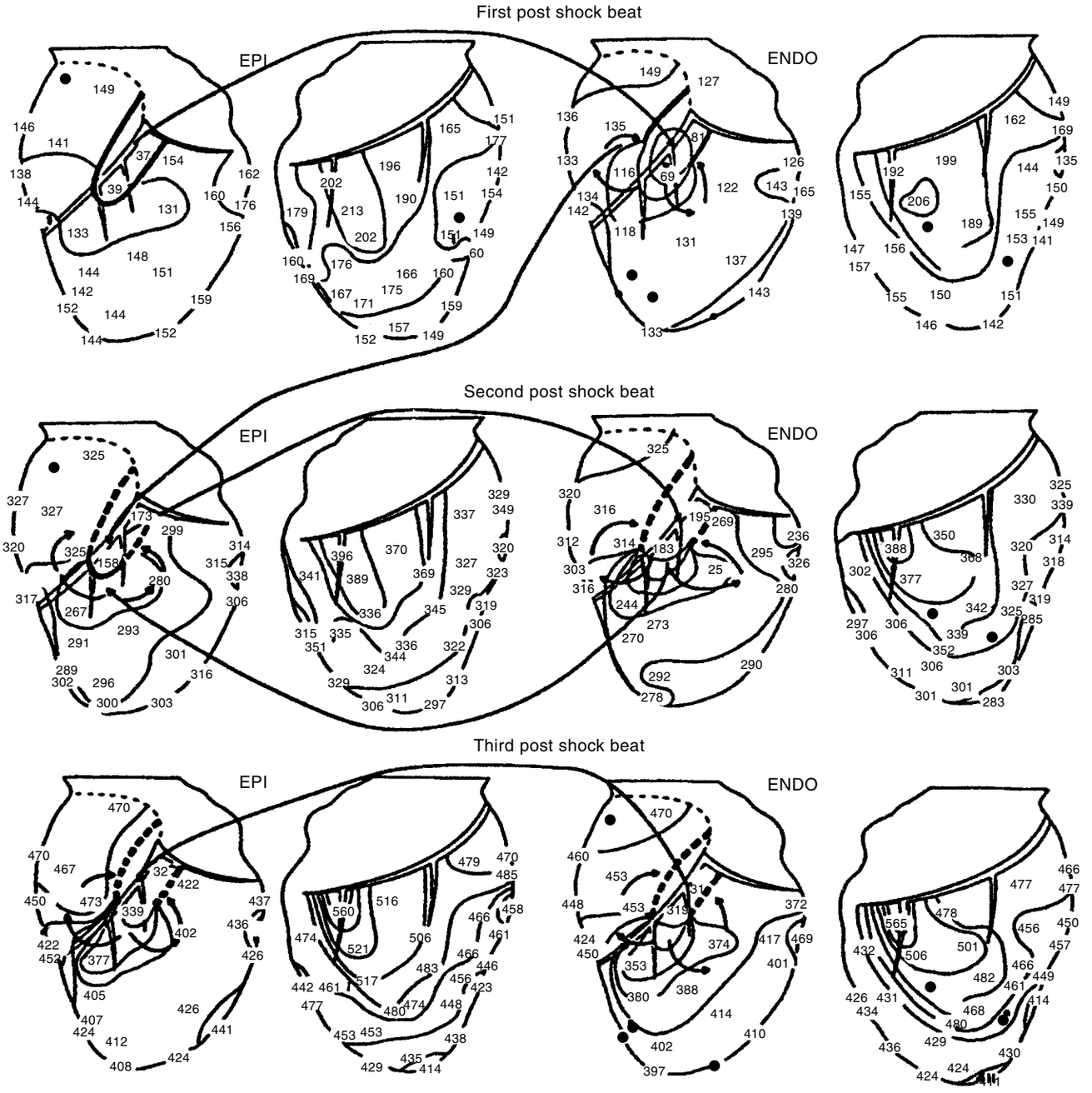

Figure 10. Postshock activation sequence. The first three cycles after the unsuccessful 500 V, 6 ms defibrillation shock shown in Fig. 9. Numbers represent activation times in milliseconds. (—) Isochronal lines, separated by 20 ms. (●) sites of electrodes where adequate recordings were not obtained. (—) represent conduction block; (---) Frame shift from one isochronal map to the next. Such dashed lines are necessary whenever a dynamic process such as reentrant activation is illustrated by a series of static maps. Reproduced with permission from The Institute of Electrical and Electronics Engineers (101).

transmembrane potential that include depolarization or hyperpolarization during the shock pulse. Several mathematical formulations have been proposed to describe which regions of the heart are depolarized and which are hyperpolarized during shocks from a particular defibrillation electrode configuration. These formulations include the cable equations, the sawtooth model (73,74), the bidomain model (75,76), and the secondary source model (77). In their simplest form, these formulations incorporate the extracellular and intracellular spaces as low resistance media and the membrane as a high resistance in parallel with a capacitance. Therefore, these simple case models incorporate only passive myocardial properties. Recently, the models have been made more realistic by the addition of active components to represent the ion chan-

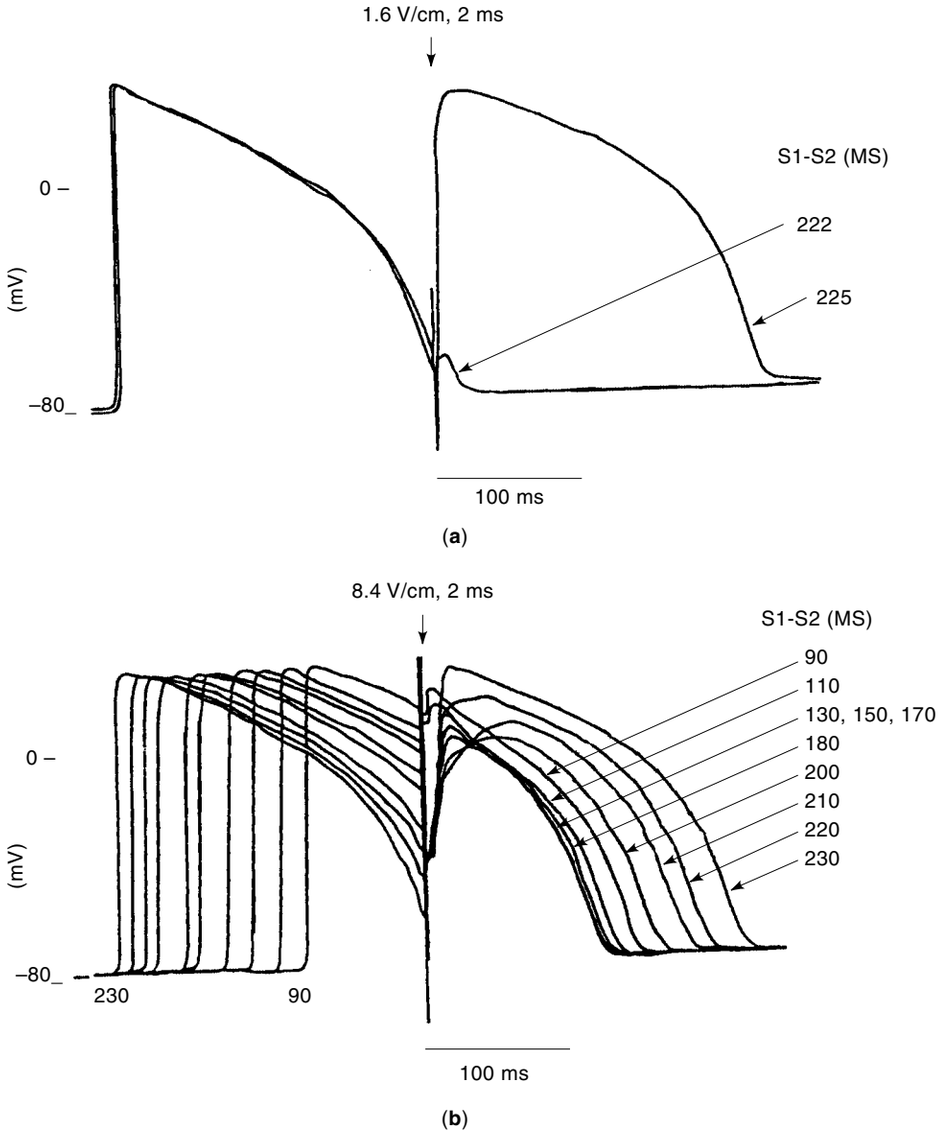

Figure 11. (a) Recordings that illustrate the response to an S2 stimulus of 1.6 V/cm oriented along the fibers. The S1–S2 stimulus intervals for each of the responses are indicated to the right of the recordings. The responses are markedly different even though the change in S2 timing was only 3 ms. An S1–S2 interval of 222 ms caused almost no response, whereas an interval of 225 ms produced a new action potential. (b) A range of action potential extensions produced by an S2 stimulus generating a potential gradient of 8.4 V/cm oriented along the long axis of the myofibers. The recordings were obtained from the same cell as (a). The action potential recordings, obtained from one cellular impairment, are aligned with the S2 time. An S1 stimulus was applied 3 ms before phase-zero of each recording. The longest and shortest S1–S2 intervals tested, 230 ms and 90 ms respectively, are indicated beneath their respective phase-zero depolarizations. The S1–S2 intervals for each response after S2 are indicated to the right. Reproduced with permission from the American Heart Association (59).

nels in the membrane. Because the extracellular space throughout the body is primarily resistive, with very little reactive components, the defibrillation shock appears in the extracellular space of the heart almost immediately and without significant distortion. For example, a shock in the form of a square wave given across the defibrillation electrodes will appear almost immediately as a square wave in the extracellular space of the heart. Because of the capacitance and the ion channels of the membrane, however, phase delays and alterations of the appearance of the shock wave occur in the transmembrane potential. For example, a square wave shock may appear as an exponential change in the transmembrane potential that reaches an asymptote (Fig. 12). Because of the nonlinear behavior of the membrane introduced by the ion channels, reversing defibrillation shock polarity does not just reverse the sign of the change in the transmembrane potential but also alters the magnitude and time-course of the change in transmembrane potential (Fig. 12).

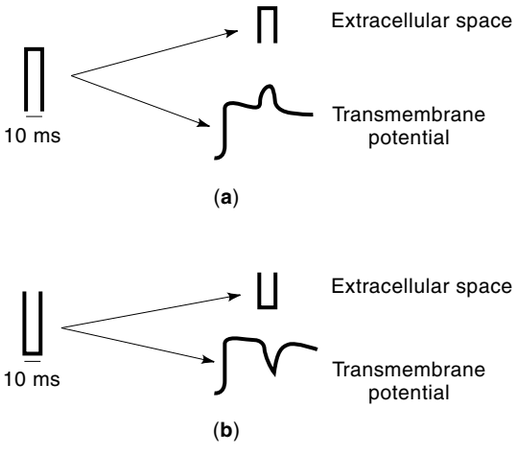

Figure 12. The effect of a square wave shock on the extracellular potential and the transmembrane potential. The square wave shock appears immediately as a relatively undistorted square wave in the extracellular space. It appears as an exponentially increasing change in the transmembrane potential. When given during the action potential plateau, as shown in the figure, the depolarization obtained when a shock of one shock polarity is delivered has a different magnitude and time-course compared to the hyperpolarization obtained when a shock of the opposite polarity is delivered. Reproduced with permission of the North American Society of Pacing and Electrophysiology (102).

The one-dimensional cable model indicates that the tissue near the anode during the defibrillation shock should be hyperpolarized, whereas the tissue near the cathode should be depolarized (78). This hyperpolarization and depolarization decreases exponentially with distance away from the electrodes. The distance at which the depolarization or hyperpolarization has decreased by 63% is called the membrane space constant. The space constant for cardiac tissue is only 0.5 mm to 1.0 mm (78,79). Therefore, the one-dimensional cable equations predict that tissue more than about 1 cm away from the defibrillation electrodes (i.e. ten space constants) should undergo almost no change in transmembrane potential caused directly by the shock field. Thus, according to one-dimensional cable theory, the shock should not be able to directly excite a new action potential at distances more than 1 cm away from the electrodes. This prediction contrasts with the experimental finding in hearts that new action potentials can be created by shocks many centimeters away from the shock electrodes (56,57).

The sawtooth formulation states that, because of the junctional resistance at the gap junctions between cells, cells in the region away from and between shock electrodes undergo hyperpolarization at the cell end facing the anode and depolarization at the cell end facing the cathode. Thus the change in transmembrane potential during the shock assumes a sawtooth distribution with each tooth of the sawtooth corresponding to an individual cell (73,74,80,81). While a sawtooth change in the transmembrane potential during a shock has been observed in single, isolated cells (82) it has never been observed in a syncytium of cardiac cells experimentally (83–86).

The bidomain formulation performs the mathematical legerdemain of representing in two or more dimensions the extracellular space as an everywhere continuous domain and the intracellular space as an everywhere continuous domain with both domains separated by the highly resistive cell membrane (87). When the ratio of the extracellular resistance along fibers to across fibers is equal to the ratio of the intracellular resistance along fibers to across fibers, the bidomain formulation predicts an effect similar to that predicted by the cable equations. In this case, hyperpolarization occurs in tissue under an extracellular anodal electrode and the magnitude of hyperpolarization decreases exponentially with distance in the direction along or across fibers according to the space constants along and across fibers. When the ratio of the intracellular resistivities is not equal to the ratio of the extracellular resistivities, however, bidomain theory differs from the results of the cable equations. An important difference is that, while hyperpolarization still occurs immediately adjacent to an anode during a shock, depolarization occurs just a few millimeters away from the electrode along the long axis of the myocardial fibers. Similarly, while depolarization occurs immediately adjacent to a cathode, hyperpolarization occurs along fibers just a few millimeters away (88–90). Several recent experiments have verified this prediction (Fig. 13) (88). The bidomain formulation does not predict a constant relationship between the extracellular potential gradient generated by the shock and the change in transmembrane potential caused by the shock. Rather, the change in transmembrane potential depends on a complex distribution of intracellular and extracellular current that involves the change over distance of the potential gradient, the distance from the electrode, and the direction of the myocardial fibers over this distance. At first glance, this prediction seems to conflict with the experimental finding that early sites of activation following failed defibrillation shocks occur in regions of lowest potential gradient and that a certain minimum potential gradient is necessary for defibrillation (50,51). However, for most commonly used defibrillation electrode configurations, the change in the potential gradient with distance is lowest in those regions in which the potential gradient itself is lowest. Therefore, these experimental findings may not necessarily be in conflict with the predictions of bidomain theory.

One limitation of the bidomain theory in its simplest form is that it does not take into consideration the discontinuities of the intracellular domain where the myocardium is crossed by connective tissue septae, blood vessels, and scar tissue. Any intracellular current that needs to cross such barriers must leave the intracellular space on one side of the barrier and reenter it on the other. Thus, depolarization should occur on one side of the barrier and hyperpolarization on the other. In other words, the connective tissue barrier will act as if it is a pair of electrodes during the shock, acting as a secondary source. For this reason, the gaps in the tissue where myocardial cells are not present have been considered to act as secondary sources. Recent studies by Gillis et al. (85) and White et al. (91) suggest that such secondary sources are important causes of depolarization and hyperpolarization throughout the myocardial tissue during a shock.

Ion Channels

The electrical activity of the heart at its most fundamental level is controlled by the ion channels located in the cell membrane. These channels selectively allow ions such as Na^+ and Ca^+ into the cardiac cell and K^+ out of the cell in response to

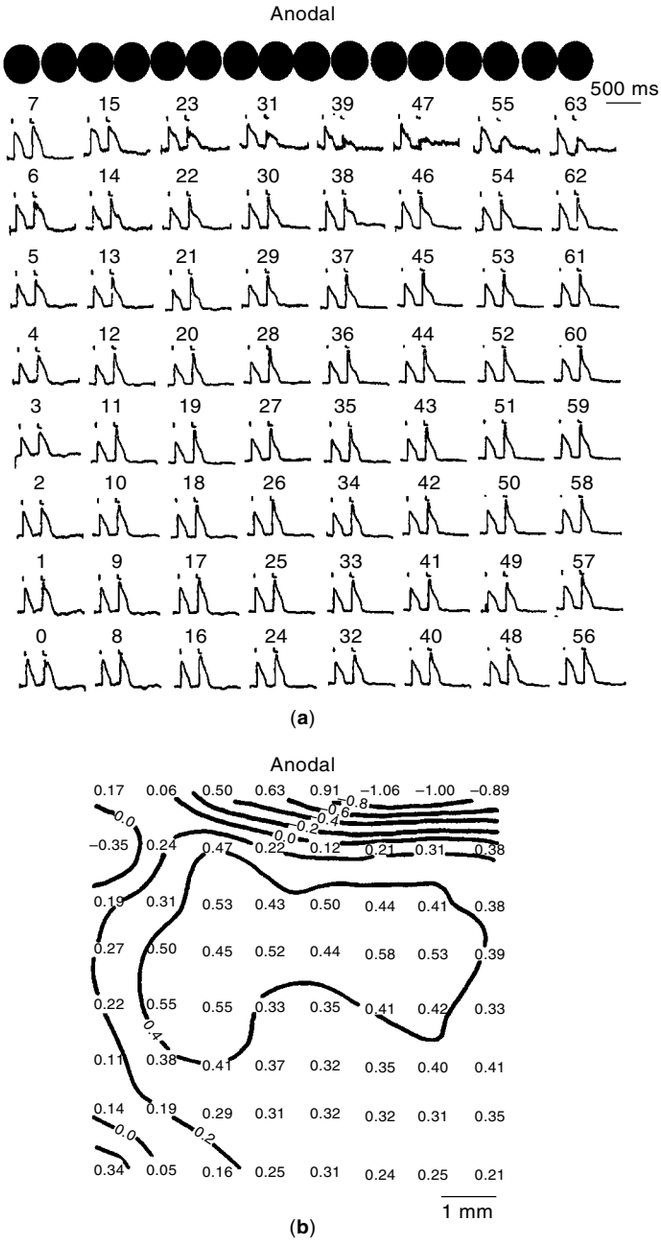

Figure 13. Fluorescence recordings showing the effect of an anodal stimulation pulse in a region adjacent to a stimulation electrode and contour plot of changes in transmembrane potential induced during the pulse. (a) Each recording shows an S1-induced action potential without an S2 stimulation pulse and then an S1-induced action potential during which an S2 stimulation pulse was applied from a line of electrode terminals (row of large spots) illustrated above the recording region. Positive changes in transmembrane potential, i.e., depolarization during S2, occurred at most spots. (b) Contour plot showing the distribution of depolarization in the recording region. The depolarization at each recording spot is given as a fraction of the amplitude of the S1-induced action potential rising phase. Contour lines are shown at intervals of 0.2 times the amplitude of the action potential rising phase. Reproduced with permission from the Biophysical Society (88).

changes in the transmembrane potential. It is known that both the fast as well as the slow Na^+ and Ca^+ channels are active during early fibrillation when defibrillation shocks are most likely to be given (92,93). It is thought that direct excitation of a new action potential by the shock is caused by activation of the sodium channels (94–96). Results from computer models have suggested that the role of the first phase of a biphasic defibrillation waveform is to hyperpolarize the cardiac cell membrane from the −65 mV that is typically its most negative transmembrane voltage during fibrillation to closer to the −80 mV to −90 mV that is the resting transmembrane voltage. This decrease in transmembrane potential is hypothesized to allow the transmembrane voltage-dependent Na^+ channels to recover. Because the Na^+ channels have recovered, the second phase of the biphasic waveform can more easily stimulate tissue and defibrillate the heart (97). These results are in direct conflict with the ideas presented earlier that the first phase of a biphasic waveform stimulates, while the second phase keeps the heart from refibrillating. More research is necessary to reconcile these results.

CONCLUSION

We have examined how various aspects of the electric shock interact with the heart at many different levels to stop fibrillation. Important aspects of the shock include its shape, the electrodes that it is delivered from, and the potential gradient field that is created in the heart because of it. The shock affects the activation sequence of the fibrillating heart, the cellular action potential, the transmembrane potential, and the cellular ion channels in a specific fashion to stop fibrillation and allow the heart to resume sinus rhythm. Understanding these interactions will allow physicians, engineers, and researchers to build more effective defibrillators and thereby extend life.

BIBLIOGRAPHY

1. AVID Trial Executive Committee, Are implantable cardioverter-defibrillators or drugs more effective in prolonging life?, *Am. J. Cardiol.,* **79**: 661–663, 1997.
2. A. J. Moss et al., Improved survival with an implanted defibrillator in patients with coronary disease at high risk for ventricular arrhythmia, *N. Engl. J. Med.,* **335**: 1933–1940, 1996.
3. M. L. Weisfeldt et al., American Heart Association report on the public access defibrillation conference, 1994. Automatic external defibrillation task force, *Circulation,* **92**: 2740–2747, 1995.
4. B. E. Gliner, Y. Murakawa, and N. V. Thakor, The defibrillation success rate versus energy relationship: Part I-Curve fitting and the most efficient defibrillation energy, *Pacing Clin. Electrophysiol.,* **13**: 326–338, 1990.
5. M. H. Lehmann et al., Defibrillation threshold testing and other practices related to AICD implantation: do all roads lead to Rome?, *Pacing Clin. Electrophysiol.,* **12**: 1530–1537, 1989.
6. W. C. McDaniel and J. C. Schuder, An up-down algorithm for estimation of the cardiac ventricular defibrillation threshold, *Med. Instrum.,* **22**: 286–292, 1988.
7. L. Wang et al., Dependent success rate of repeated shocks at DFT determined by binary search, *Pacing Clin. Electrophysiol.,* **20**: 1169, 1997.
8. J. D. Bourland, W. A. Tacker, Jr., and L. A. Geddes, Strength-duration curves for trapezoidal waveforms of various tilts for

transchest defibrillation in animals, *Med. Instrum.,* **12**: 38–41, 1978.

9. R. A. Malkin, T. C. Pilkington, and D. S. Burdick, Optimizing existing defibrillation thresholding techniques, presented at *Annu. Int. Conf. IEEE Eng. Med. Biol. Soc.,* Piscataway, NJ, 1990.
10. R. A. Malkin et al., Estimating the 95% effective defibrillation dose, *IEEE Trans. Biomed. Eng.,* **40**: 256–265, 1993.
11. F. P. van Rugge, L. H. Savalle, and M. J. Schalij, Subcutaneous single-incision implantation of cardioverter-defibrillators under local anesthesia by electrophysiologists in the electrophysiology laboratory, *Am. J. Cardiol.,* **81**: 302–305, 1998.
12. R. A. S. Cooper et al., Comparison of multiple biphasic and monophasic waveforms for internal cardioversion of atrial fibrillation in humans, *Circulation,* **90**: 1–13, 1994.
13. R. A. S. Cooper, E. E. Johnson, and M. Wharton, Internal atrial defibrillation in humans. Improved efficacy of biphasic waveforms and the importance of phase duration, *Circulation,* **95**: 1487–1496, 1997.
14. C.-P. Lau and N.-S. Lok, A comparison of transvenous atrial defibrillation of acute and chronic atrial fibrillation and the effect of intravenous Sotalol on human atrial defibrillation threshold, *Pacing Clin. Electrophysiol.,* **20**: 2442–2452, 1997.
15. A. Heisel et al., Low-energy transvenous cardioversion of atrial fibrillation using a single atrial lead system, *JCW,* **8**: 607–614, 1997.
16. G. Tomassoni et al., Testing different biphasic waveforms and capacitances: effect on atrial defibrillation threshold and pain perception, *J. Am. Coll. Cardiol.,* **28**: 695–699, 1996.
17. R A. S. Cooper, W. M. Smith, and R. E. Ideker, Dual current pathways for internal atrial defibrillation in sheep: marked reduction in defibrillation threshold, *J. Am. Coll. Cardiol.,* **29**: 195A, 1997.
18. W. D. Weaver et al., Ventricular defibrillation—a comparative trial using 175-J and 320-J shocks, *N. Engl. J. Med.,* **307**: 1101–1106, 1982.
19. G. H. Bardy et al., Multicenter comparison of truncated biphasic shocks and standard damped sine wave monophasic shocks for transthoracic ventricular defibrillation. Transthoracic Investigators, *Circulation,* **94**: 2507–2514, 1996.
20. H. L. Greene et al., Comparison of monophasic and biphasic defibrillating pulse waveforms for transthoracic cardioversion, *Am. J. Cardiol.,* **75**: 1135–1139, 1995.
21. F. J. Claydon, III et al., A volume conductor model of the thorax for the study of defibrillation fields, *IEEE Trans. Biomed. Eng.,* **35**: 981–992, 1988.
22. W. J. Karlon, S. R. Eisenberg, and J. L. Lehr, Effects of paddle placement and size on defibrillation current distribution: a three-dimensional finite element model, *IEEE Trans. Biomed. Eng.,* **40**: 246–255, 1993.
23. B. B. Lerman and O. C. Deale, Relation between transcardiac and transthoracic current during defibrillation in humans, *Circ. Res.,* **67**: 1420–1426, 1990.
24. R E. Kerber et al., Energy, current, and success in defibrillation and cardioversion: clinical studies using an automated impedance-based method of energy adjustment, *Circulation,* **77**: 1038–1046, 1988.
25. B. B. Lerman, J. P. DiMarco, and D. E. Haines, Current-based versus energy-based ventricular defibrillation: a prospective study, *J. Am. Coll. Cardiol.,* **12**: 1259–1264, 1988.
26. J. E. Poole et al., Low-energy impedance-compensating biphasic waveforms terminate ventricular fibrillation at high rates in victims of out-of-hospital cardiac arrest. LIFE Investigators, *J. Cardiovasc. Electrophysiol.,* **8**: 1373–1385, 1997.
27. E. G. Dixon et al., Decreased defibrillation thresholds with large contoured patch electrodes in dogs, *J. Am. Coll. Cardiol.,* **9**: 143A, 1987.
28. S. A. Feeser et al., Strength-duration and probability of success curves for defibrillation with biphasic waveforms, *Circulation,* **82**: 2128–2141, 1990.
29. G. P. Walcott et al., Choosing the optimal monophasic and biphasic waveforms for ventricular defibrillation, *J. Cardiovasc. Electrophysiol.,* **6**: 737–750, 1995.
30. M. W. Kroll, A minimal model of the single capacitor biphasic defibrillation waveform, *Pacing Clin. Electrophysiol.,* **17**: 1782–1792, 1994.
31. C. D. Swerdlow, W. Fan, and J. E. Brewer, Charge-burping theory correctly predicts optimal ratios of phase duration for biphasic defibrillation waveforms, *Circulation,* **94**: 2278–2284, 1996.
32. H. A. Blair, On the intensity-time relations for stimulation by electric currents. II, *J. Gen. Physiol.,* **15**: 731–755, 1932.
33. L. Lapicque, in *L'Excitabilite en Fonction du Temps.* Paris: Libraire J. Gilbert, 1926.
34. G. A. Mouchawar et al., Ability of the Lapicque and Blair strength-duration curves to fit experimentally obtained data from the dog heart, *IEEE Trans. Biomed. Eng.,* **36**: 971–974, 1989.
35. W. Irnich, The fundamental law of electrostimulation and its application to defibrillation, *Pacing Clin. Electrophysiol.,* **13**: 1433–1447, 1990.
36. M. W. Kroll, A minimal model of the monophasic defibrillation pulse, *Pacing Clin. Electrophysiol.,* **16**: 769–777, 1993.
37. R. J. Sweeney et al., Defibrillation using a high-frequency series of monophasic rectangular pulses: observations and model predictions, *J. Cardiovasc. Electrophysiol.,* **7**: 134–143, 1996.
38. J. C. Schuder et al., Transthorecic defibrillation in the dog with truncated and untruncated exponential waveforms, *Trans. IEEE Biomed. Eng.* **18** (6): 410–415, 1997.
39. M. R. Gold and S. R. Shorofsky, Strength-duration relationship for human transvenous defibrillation, *Circulation,* **96**: 3517–3520, 1997.
40. G. P. Walcott et al., Comparison of damped sinusoidal and truncated exponential waveforms for external defibrillation, *J. Am. Coll. Cardiol.,* **27**: 237A, 1996.
41. M. T. Harbinson et al., Rounded biphasic waveform reduces energy requirements for transvenous catheter cardioversion of atrial fibrillation and flutter, *Pacing Clin. Electrophysiol.,* **20**: 226–229, 1997.
42. R. E. Hillsley et al., Is the second phase of a biphasic defibrillation waveform the defibrillating phase?, *Pacing Clin. Electrophysiol.,* **16**: 1401–1411, 1993.
43. J. C. Schuder, G. A. Rahmoeller, and H. Stoeckle, Transthoracic ventricular defibrillation with triangular and trapezoidal waveforms, *Circ. Res.,* **19**: 689–694, 1966.
44. G. P. Walcott et al., Choosing the optimum monophasic and biphasic waveforms for defibrillation, *Pacing Clin. Electrophysiol.,* **17**: 789, 1994.
45. D. S. Echt et al., Influence of ventricular fibrillation duration on defibrillation energy in dogs using bidirectional pulse discharges, *PACE,* **11**: 1315–1323, 1988.
46. G. H. Bardy et al., A prospective, randomized evaluation of effect of ventricular fibrillation duration on defibrillation thresholds in humans, *JACC,* **13** (6): 1362–1366, 1989.
47. J. L. Jones et al., Increasing fibrillation duration enhances relative asymmetrical biphasic versus monophasic defibrillator waveform efficacy, *CIRCRES,* **67**: 376–384, 1990.

48. O. Fujimura et al., Effects of time to defibrillation and subthreshold preshocks on defibrillation success in pigs, *PACE,* **12**(2): 358–365, 1989.
49. R. A. Winkle et al., Effect of duration of ventricular fibrillation on defibrillation efficacy in humans, *CIRC,* **81**: 1477–1481, 1990.
50. J. M. Wharton et al., Cardiac potential and potential gradient fields generated by single, combined, and sequential shocks during ventricular defibrillation, *Circulation,* **85**: 1510–1523, 1992.
51. X. Zhou et al., Epicardial mapping of ventricular defibrillation with monophasic and biphasic shocks in dogs, *Circ. Res.,* **72**: 145–160, 1993.
52. N. Shibata et al., Epicardial activation following unsuccessful defibrillation shocks in dogs, *Am. J. Physiol.,* **255**: H902–H909, 1988.
53. P.-S. Chen et al., Comparison of activation during ventricular fibrillation and following unsuccessful defibrillation shocks in open chest dogs, *Circ. Res.,* **66**: 1544–1560, 1990.
54. R. G. Walker et al., Sites of earliest activation following transvenous defibrillation, *Circulation,* **90**: 1–447, 1994.
55. R. G. Walker, W. M. Smith, and R. E. Ideker, Activation patterns following defibrillation with different waveforms, *Pacing Clin. Electrophysiol.,* **18** (part II): 835, 1995.
56. P. G. Colavita et al., Determination of effects of internal countershock by direct cardiac recordings during normal rhythm, *Am. J. Physiol.,* **250**: H736–H740, 1986.
57. K. F. Kwaku and S. M. Dillon, Shock-induced depolarization of refractory myocardium prevents wave-front propagation in defibrillation, *Circ. Res.,* **79**: 957–973, 1996.
58. C. Y. Kao and B. F. Hoffman, Graded and decremental response in heart muscle fibers, *Am. J. Physiol.,* **194**: 187–196, 1958.
59. S. B. Knisley, W. M. Smith, and R. E. Ideker, Effect of field stimulation on cellular repolarization in rabbit myocardium: implications for reentry induction, *Circ. Res.,* **70**: 707–715, 1992.
60. S. B. Knisley and B. C. Hill, Optical recordings of the effect of electrical stimulation on action potential repolarization and the induction of reentry in two-dimensional perfused rabbit epicardium, *Circulation,* **88** (part I): 2402–2414, 1993.
61. J. F. Swartz et al., Conditioning prepulse of biphasic defibrillator waveforms enhances refractoriness to fibrillation wavefronts, *Circ. Res.,* **68**: 438–449, 1991.
62. R. J. Sweeney et al., Ventricular refractory period extension caused by defibrillation shocks, *Circulation,* **82**: 965–972, 1990.
63. S. M. Dillon, Optical recordings in the rabbit heart show that defibrillation strength shocks prolong the duration of depolarization and the refractory period, *Circ. Res.,* **69**: 842–856, 1991.
64. S. M. Dillon and R. Mehra, Prolongation of ventricular refractoriness by defibrillation shocks may be due to additional depolarization of the action potential, *J. Cardiovasc. Electrophysiol.,* **3**: 442–456, 1992.
65. S. M. Dillon, Synchronized repolarization after defibrillation shocks: a possible component of the defibrillation process demonstrated by optical recordings in rabbit heart, *Circulation,* **85**: 1865–1878, 1992.
66. P.-S. Chen, P. D. Wolf, and R. E. Ideker, Mechanism of cardiac defibrillation: a different point of view, *Circulation,* **84**: 913–919, 1991.
67. O. Tovar and L. Tung, Electroporation of cardiac cell membranes with monophasic or biphasic rectangular pulses, *Pacing Clin. Electrophysiol.,* **14**: 1887–1892, 1991.
68. S. B. Knisley and A. O. Grant, Asymmetrical electrically induced injury of rabbit ventricular myocytes, *J. Mol. Cell. Cardiol.,* **27**: 1111–1122, 1995.
69. E. N. Moore and J. F. Spear, Electrophysiologic studies on the initiation, prevention, and termiation of ventricular fibrillation, in D. P. Zipes and J. Jalife (eds.), *Cardiac Electrophysiology and Arrhythmias,* Orlando: Grune & Stratton, 1985, pp. 315–322.
70. S. Yabe et al., Conduction disturbances caused by high current density electric fields, *Circ. Res.,* **66**: 1190–1203, 1990.
71. J. L. Jones and R. E. Jones, Decreased defibrillator-induced dysfunction with biphasic rectangular waveforms, *Am. J. Physiol.,* **247**: H792–H796, 1984.
72. J. C. Eason, *Membrane polarization in a bidomain model of electrical field stimulation of myocardial tissue,* Duke Univ., Durham, NC, 1995.
73. R. Plonsey and R. C. Barr, Inclusion of junction elements in a linear cardiac model through secondary sources: application to defibrillation, *Med. Biol. Eng. Comput.,* **24**: 137–144, 1986.
74. R. Plonsey and R. C. Barr, Effect of microscopic and macroscopic discontinuities on the response of cardiac tissue to defibrillating (stimulating) currents, *Med. Biol. Eng. Comput.,* **24**: 130–136, 1986.
75. N. G. Sepulveda, B. J. Roth, and J. P. Wikswo, Jr., Current injection into a two-dimensional anisotropic bidomain, *Biophys. J.,* **55**: 987–999, 1989.
76. N. Trayanova, A bidomain model for ring stimulation of a cardiac strand, *IEEE Trans. Biomed. Eng.,* **41**: 393–397, 1994.
77. N. A. Trayanova, T. C. Pilkington, and C. S. Henriquez, A periodic bidomain model for cardiac tissue, presented at *Annu. Int. Conf. IEEE Eng. Med. Biol. Soc.,* Piscataway, NJ, 1991.
78. S. Weidmann, Electrical constants of trabecular muscle from mammalian heart, *J. Physiol.,* **210**: 1041–1054, 1970.
79. A. G. Kléber and C. B. Riegger, Electrical constants of arterially perfused rabbit papillary muscle, *J. Physiol.,* **385**: 307–324, 1987.
80. W. Krassowska et al., Potential distribution in three-dimensional periodic myocardium: part II, Application to extracellular stimulation, *IEEE Trans. Biomed. Eng.,* **37**: 267–284, 1990.
81. W. Krassowska, T. C. Pilkington, and R. E. Ideker, Potential distribution in three-dimensional myocardium: part I, Solution with two-scale asymptotic analysis, *IEEE Trans. Biomed. Eng.,* **37**: 252–266, 1990.
82. S. B. Knisley et al., Optical measurements of transmembrane potential changes during electric field stimulation of ventricular cells, *Circ. Res.,* **72**: 255–270, 1993.
83. X. Zhou et al., Optical transmembrane potential measurements during defibrillation-strength shocks in perfused rabbit hearts, *Circ. Res.,* **77**: 593–602, 1995.
84. X. Zhou et al., Spatial changes in transmembrane potential during a shock, *Pacing Clin. Electrophysiol.,* **18** (part II): 935, 1995.
85. A. M. Gillis et al., Microscopic distribution of transmembrane potential during application of defibrillatory shocks in strands and monolayers of cultured myocytes, *Pacing and Clin. Electrophysiol.,* **19**: 570, 1996.
86. J. P. Wikswo Jr., Tissue anisotropy, the cardiac bidomain, and the virtual cathode effect, in D. P. Zipes and J. Jalife, (eds.), *Cardiac Electrophysiology: From Cell to Bedside,* 2nd ed. Philadelphia: W. B. Saunders, 1995, pp. 348–362.
87. L. Tung, *A bidomain model for describing ischemic myocardial DC potentials,* MIT, Cambridge, MA, 1978.
88. S. B. Knisley, B. C. Hill, and R. E. Ideker, Virtual electrode effects in myocardial fibers, *Biophys. J.,* **66**: 719–728, 1994.

89. S. B. Knisley, Transmembrane voltage changes during unipolar stimulation of rabbit ventricle, *Circ. Res.,* **77**: 1229–1239, 1995.
90. J. P. Wikswo, Jr., S.-F. Lin, and R. A. Abbas, Virtual electrodes in cardiac tissue: A common mechanism for anodal and cathodal stimulation, *Biophys. J.,* **69**: 2195–2210, 1995.
91. J. B. White et al., Myocardial discontinuities: a substrate for producing virtual electrodes to increase directly excited areas of the myocardium by shocks, *Circulation,* **97**: 1998.
92. T. Akiyama, Intracellular recording of in situ ventricular cells during ventricular fibrillation, *Am. J. Physiol.,* **240**: H465–H471, 1981.
93. X. Zhou et al., Existence of both fast and slow channel activity during the early stage of ventricular fibrillation, *Circ. Res.,* **70**: 773–786, 1992.
94. J. L. Jones and R. E. Jones, Threshold reduction with biphasic defibrillator waveforms: role of excitation channel recovery in a computer model of the ventricular action potential, *J. Electrocardiol.,* **23**: 30–35, 1990.
95. L. Tung and J.-R. Borderies, Analysis of electric field stimulation of single cardiac muscle cells, *J. Physiol.,* **63**: 371–386, 1992.
96. X. Zhou et al., Transmembrane potential changes caused by shocks in guinea pig papillary muscle, *Am. J. Physiol.,* **271**: H2536–H2546, 1996.
97. J. L. Jones and R. E. Jones, Threshold reduction with biphasic defibrillator waveforms: role of excitation channel recovery in computer model of the ventricular action potential, *J. Electrocardiol.,* **23**: 30–35, 1991.
98. T. D. Valenzuela et al., Estimating effectiveness of cardiac arrest intervention: a logistic regression survival model, *Circulation,* **96**: 3308–3313, 1997.
99. J. C. Schuder et al., Transthoracic ventricular defibrillation in the 100 kg calf with untruncated and truncated exponential stimuli, *IEEE Trans. Biomed. Eng.,* **BME 27**: 37–43, 1980.
100. N. L. Gurvich and V. A. Markarychev, Defibrillation of the heart with biphasic electrical impulses, *Kardiologiia,* **7**: 109–112, 1967.
101. A. S. L. Tang et al., Measurement of defibrillation shock potential distributions and activation sequences of the heart in three-dimensions, *Proc. IEEE,* **76**: 1176–1186, 1988.
102. G. P. Walcott et al., On the mechanism of ventricular defibrillation, *Pacing Clin. Electrophysiol.,* **20**: 422–431, 1997.

GREGORY P. WALCOTT
RAYMOND E. IDEKER
University of Alabama at Birmingham

DEGREE PROGRAMS. See ELECTRICAL ENGINEERING CURRICULA.